Tumor invasion in the absence of epithelial-mesenchymal transition: Podoplanin-mediated remodeling of the actin cytoskeleton

Andreas Wicki,[1] François Lehembre,[1] Nikolaus Wick,[2] Brigitte Hantusch,[2] Dontscho Kerjaschki,[2] and Gerhard Christofori[1,*]

[1] Institute of Biochemistry and Genetics, Department of Clinical-Biological Sciences, Center of Biomedicine, University of Basel, 4058 Basel, Switzerland
[2] Clinical Institute for Pathology, Medical University of Vienna, 1090 Wien, Austria
*Correspondence: gerhard.christofori@unibas.ch

Summary

The expression of podoplanin, a small mucin-like protein, is upregulated in the invasive front of a number of human carcinomas. We have investigated podoplanin function in cultured human breast cancer cells, in a mouse model of pancreatic β cell carcinogenesis, and in human cancer biopsies. Our results indicate that podoplanin promotes tumor cell invasion in vitro and in vivo. Notably, the expression and subcellular localization of epithelial markers are unaltered, and mesenchymal markers are not induced in invasive podoplanin-expressing tumor cells. Rather, podoplanin induces collective cell migration by filopodia formation via the downregulation of the activities of small Rho family GTPases. In conclusion, podoplanin induces an alternative pathway of tumor cell invasion in the absence of epithelial-mesenchymal transition (EMT).

Introduction

A critical step in the development of a malignant tumor is characterized by a gain in the tumor cells' migratory and invasive capabilities. In the past years, a number of molecular mechanisms have been identified by which normal and transformed cells become migratory and invasive during embryonic development and during carcinogenesis. These processes include induction of cellular migration and invasion by receptor tyrosine kinase-mediated signal transduction pathways, by changes in cell adhesion, and by the activation of small GTPases of the Rho family, which in turn leads to the reorganization of the actin cytoskeleton (reviewed by Cavallaro and Christofori, 2004; Grunert et al., 2003; Sahai and Marshall, 2002; Thiery, 2002). Yet, the molecular details of how tumor cells acquire these malignant properties are still poorly understood.

Oncogenic events in tumor cells as well as growth factors secreted by tumor and stromal cells induce a multistep process termed epithelial-mesenchymal transition (EMT; reviewed in Grunert et al., 2003; Siegel and Massague, 2003; Thiery, 2002). During EMT, cells progressively redistribute or downregulate their apical and basolateral epithelial-specific proteins, such as E-cadherin, catenins, and cytokeratins, and re-express mesenchymal molecules, such as vimentin, fibronectin, and N-cadherin. These changes lead to the abrogation of cell-cell contacts and the gain of cell motility necessary for invasion. EMT of in vitro cultured cells resembles the metastatic process observed in patients, although this hypothesis is still under debate (Grunert et al., 2003).

Previously, our laboratory has demonstrated that loss of E-cadherin function is a rate-limiting step during the transition from adenoma to carcinoma (Perl et al., 1998). Concomitant with the loss of E-cadherin, a strong upregulation of N-cadherin expression is observed. Such a cadherin switch has been previously described during the progression of various cancer types and is thought to be necessary for tumor cells to gain invasive properties (Cavallaro et al., 2002; Hsu et al., 1996). Migration and invasion of tumor cells are also promoted by the loss of interaction of adherens junctions with the cytoskeleton, subsequent changes in the activities of Rho family small GTPases (most prominently Rac1, Cdc42, and RhoA), and the concomitant reorganization of the actin cytoskeleton (Noren et al., 2000; Sahai and Marshall, 2002).

Despite the major progress in the understanding of the molecular processes underlying EMT and tumor progression, a number

SIGNIFICANCE

In most epithelial cancers, the expression of E-cadherin is lost during the transition from adenoma to carcinoma. Here, we report a molecular pathway of tumor progression that does not involve the loss of E-cadherin function or epithelial-mesenchymal transition: podoplanin, which is frequently upregulated in the invasive front of human cancers, induces tumor cell migration and invasion in breast cancer cells in vitro and in a mouse model of tumorigenesis in vivo without dissolving E-cadherin-mediated junctional complexes. Podoplanin induces the formation of filopodia by modulating the activities of Rho-family GTPases, which ultimately leads to collective cell invasion, a phenotype often observed in human carcinoma. These results raise important questions about diagnosing malignant disease and designing adequate antimetastatic therapies.

of questions still remain unresolved. For example, a significant number of cancers, including certain subtypes of breast and ovarian cancers, are by pathological criteria characterized as invasive and malignant, yet they do not lose E-cadherin expression. Moreover, full EMT is rarely observed in biopsies from cancer patients.

Recently, podoplanin (PA2.26, T1α-2, aggrus), a small, 38 kDa mucin-type transmembrane glycoprotein, has been implicated in tumor progression. The expression of podoplanin is upregulated in a number of different cancers, including squamous cell carcinoma of the oral cavity, lung, and skin, granulosa cell tumors, and mesothelioma (Kato et al., 2005; Kimura and Kimura, 2005; Martin-Villar et al., 2005; Schacht et al., 2005). Podoplanin is expressed in human kidney podocytes and is homologous to T1α-2, an antigen expressed on the apical surface of alveolar type I cells (Rishi et al., 1995). Other podoplanin homologs include OTS-8, RTI40, gp 38, canine gp 40, human gp 36, and murine PA 2.26 (Farr et al., 1992; Gonzalez and Dobbs, 1998; Martin-Villar et al., 2005; Nose et al., 1990; Zimmer et al., 1997; Zimmer et al., 1999). Since podoplanin is expressed on lymphatic endothelium but not on blood vessel endothelium, it is also widely used as a specific marker for lymphatic endothelial cells and lymphangiogenesis (Breiteneder-Geleff et al., 1999). Podoplanin-deficient mice die at birth due to respiratory failure, exhibiting a phenotype of dilated, malfunctioning lymphatic vessels and lymphedema (Schacht et al., 2003). Yet, the physiological function of podoplanin is still unknown. Also, the functional contribution of podoplanin to tumor progression has remained elusive. Early experiments addressing this issue have revealed that podoplanin colocalizes with ezrin, an ERM-protein (ezrin-radixin-moesin), at the cellular membrane, and that podoplanin promotes relocalization of ezrin to filopodia-like structures and reduces cell-cell adhesiveness (Martin-Villar et al., 2005). In this context, it is important to note that ezrin itself has been regarded as a tumor promoter, since its overexpression can enhance tumor progression in various cancer models (Hunter, 2004; McClatchey, 2003).

Here, we have investigated the functional role of podoplanin during tumor progression in vitro and in vivo. To this end, we generated transgenic mouse lines expressing podoplanin under the control of the rat insulin promoter in the β cells of islets of Langerhans (Rip1Podo). We then crossed Rip1Podo mice into the Rip1Tag2 transgenic mouse model of pancreatic β cell carcinogenesis (Hanahan, 1985). In Rip1Tag2 transgenic mice, Simian Virus 40 large and small T antigen are expressed under the control of the rat insulin promoter. These mice reproducibly develop tumors in a multistage tumorigenesis pathway involving islet hyperplasia, the formation of new blood vessels (angiogenesis), and, finally, β cell adenomas and carcinomas (Christofori et al., 1994; Folkman et al., 1989; Perl et al., 1998). The impact of forced expression of podoplanin on tumor progression in double transgenic Rip1Podo;Rip1Tag2 mice was then compared to single transgenic Rip1Tag2 mice. In addition, we established MCF7 breast cancer cell lines that stably expressed podoplanin and analyzed podoplanin-mediated changes in various cellular parameters, including cell migration and invasion. Finally, we employed tumor biopsies from cancer patients to correlate podoplanin expression with tumor invasion. Together, the results from these in vivo and in vitro experiments indicate that podoplanin employs a novel molecular pathway of inducing collective tumor cell invasion in the absence of profound changes in junctional adhesion complexes or EMT.

Results

Generation of Rip1Podo transgenic mice

We have generated transgenic mice expressing murine podoplanin specifically in the insulin-producing β cells of the pancreatic islets of Langerhans. A cDNA encoding murine podoplanin was cloned between a rat insulin II promoter fragment and a human growth hormone intron and polyadenylation signal, thus targeting podoplanin expression to pancreatic β cells (Hanahan, 1985). Six independent transgenic mouse lines were established that exhibited stable transmission of the transgene to their progeny. Rip1Podo transgenic mice were viable, normoglycemic, and fertile. Analysis of transgene expression was examined at the RNA level by RT-PCR (data not shown) and by immunofluorescent staining of histological sections of pancreata of transgenic mice (Figure S1). Strong podoplanin expression was detected in all islets of several Rip1Podo mouse lines, but not in nontransgenic littermate controls. In the exocrine pancreas, the only detectable podoplanin protein could be attributed to lymphatic vessels.

Histopathological analyses of both adult and newborn pancreas did not reveal any significant differences in islet morphology between Rip1Podo mice and nontransgenic littermate controls, although transgenic podoplanin expression could be detected already in islets of newborn mice. Also, the presence and distribution of cells producing insulin, glucagon, pancreatic polypeptide, and somatostatin was unaltered regardless of the age of the mice (data not shown). Moreover, the expression of podoplanin affected neither blood vessel density and morphology within the islets of Langerhans nor the morphology and distribution of lymphatic vessels, which were exclusively found in the exocrine pancreas in control and in Rip1Podo mice (data not shown).

Podoplanin promotes invasion of β cell tumors

We next crossed Rip1Podo mice with Rip1Tag2 mice in order to generate double-transgenic Rip1Podo;Rip1Tag2 mice. Both single and double-transgenic mice were kept in a C57Bl/6 background. Single-transgenic Rip1Tag2 mice were used as experimental controls to identify podoplanin-specific effects on tumor progression in double-transgenic Rip1Podo;Rip1Tag2 mice. Obvious physiological or pathological differences or changes in life span were not detected between single-transgenic and double-transgenic mice.

Mice were sacrificed between the age of 12 and 13 weeks, a time point when Rip1Tag2 mice succumb to hypoglycemia. Histological staging and grading was performed on paraffin sections of pancreata from double-transgenic Rip1Podo; Rip1Tag2 and from single-transgenic Rip1Tag2 mice on the basis of the 2001 WHO classification of rodent tumors (Mohr et al., 2001). Islets and β cell tumors were staged into normal islets, hyperplastic islets, adenoma (noninvasive tumor), or carcinoma (invasive tumor) with 3 grades: grade 1, invasive tumors with the invading front comprising less than 20% of the entire tumor periphery; grade 2, carcinoma with more than 20%; grade 3, carcinoma with high-grade invasion, nuclear atypia, and anaplasia. Detailed analysis of pancreata from 18 double-transgenic and 13 single-transgenic mice revealed that podoplanin-expressing mice exhibited a higher incidence of carcinomas than single-transgenic controls (Figure 1A). In particular, the number of grade 2 carcinomas was significantly higher in Rip1Podo;Rip1Tag2

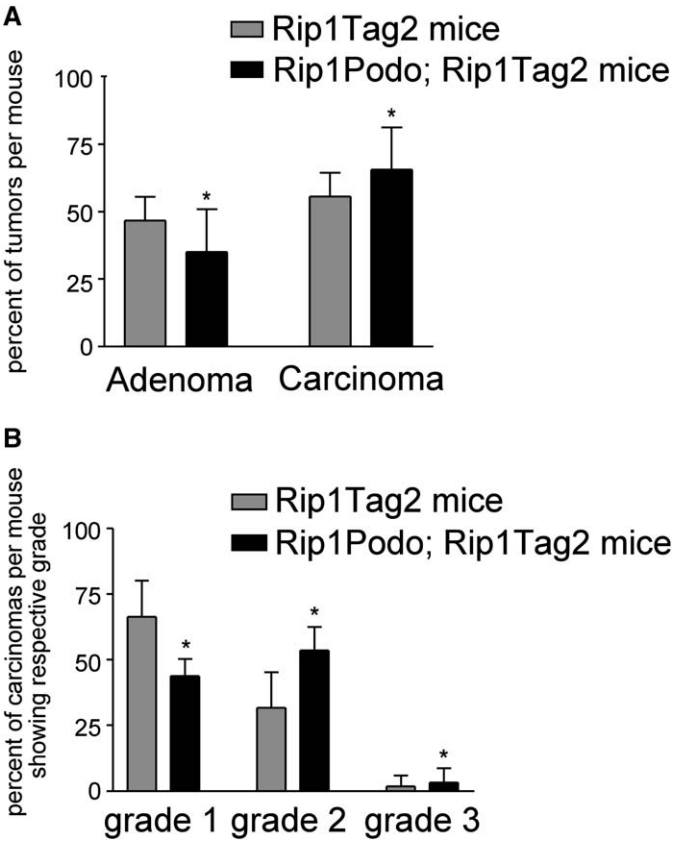

Figure 1. Accelerated tumor progression in Rip1Podo;Rip1Tag2 double-transgenic mice

A: Distribution of adenomas and carcinomas in Rip1Podo;Rip1Tag2 double-transgenic and Rip1Tag2 single-transgenic mice. The incidence of adenomas is reduced from 48% in Rip1Tag2 to 33% in Rip1Podo;Rip1Tag2 mice. Conversely, the incidence of carcinomas is increased in Rip1Podo;Rip1Tag2 mice (*p = 0.04, Fisher's exact test). Data are shown as mean ± SEM.

B: Grading of tumor stages in Rip1Podo;Rip1Tag2 double-transgenic and Rip1Tag2 single-transgenic mice. Carcinomas were graded according to the size of the invading front and the degree of nuclear atypia (see text). Invasiveness of tumors in double-transgenic Rip1Podo;Rip1Tag2 mice was significantly enhanced (*p = 0.005, chi-square test). Data are shown as mean ± SEM.

mice (Figure 1B). Lymph node and distant organ metastasis were not detected in either single-transgenic or double-transgenic mice.

Expression of podoplanin during Rip1Tag2 tumorigenesis affected neither tumor incidences nor tumor volumes. Moreover, the rates of tumor cell apoptosis and tumor cell proliferation, as assessed by TUNEL and BrdU incorporation assays, respectively, were not significantly altered by podoplanin (Figures S2A and S2B). Since podoplanin has been reported to play a role in the development of lymphatic vessels (Schacht et al., 2003), we also examined the morphology and density of blood and lymphatic vessels in Rip1Podo;Rip1Tag2 double-transgenic mice by immunohistochemical staining with antibodies against CD31 and LYVE-1, respectively (Figures S2C–S2F). No apparent difference in blood and lymphatic vessel morphology could be detected, and quantitation of vessel densities did not reveal any significant impact of podoplanin expression on blood vessel angiogenesis and lymphangiogenesis during tumor progression (data not shown). From these analyses, we conclude that podoplanin promotes tumor invasiveness in vivo by conferring migratory and invasive properties to tumor cells without affecting other tumor growth parameters.

Podoplanin bypasses EMT during Rip1Tag2 tumor progression

We have previously demonstrated that the loss of E-cadherin expression is a rate-limiting step in the transition from adenoma to carcinoma during Rip1Tag2 tumorigenesis (Perl et al., 1998). To assess whether podoplanin modulates the transition from adenoma to carcinoma by affecting the epithelial character of tumor cells, E-cadherin expression in tumors from Rip1Tag2 mice and Rip1Podo;Rip1Tag2 mice was analyzed by immunofluorescence staining with antibodies against E-cadherin. As expected, in Rip1Tag2 control mice, E-cadherin staining was absent in invasive tumors (Figure 2A). In contrast, in podoplanin-expressing tumors, strong E-cadherin staining could be observed at the membranes of most tumor cells (Figure 2B). Double staining for the expression of E-cadherin and podoplanin revealed a strong colocalization of E-cadherin and podoplanin at cell-cell junctions, even of invasive tumor cells (Figures 2C and 2D). To verify whether E-cadherin is present at the tumor rim and in the invading front, the expression of E-cadherin was also analyzed by immunohistochemical staining on frozen sections. In tumors from Rip1Tag2 control mice, E-cadherin was undetectable in invasive tumor cells (Figure 2E). In contrast, E-cadherin was still present in podoplanin-expressing tumor cells in the invading front of carcinomas (Figure 2F). The majority of carcinomas in the podoplanin overexpressing mice were positive for E-cadherin, whereas most carcinomas in control mice had lost E-cadherin expression (Figure 2G). This surprising observation suggests that in the presence of podoplanin the induction of tumor invasion is not dependent on the loss of E-cadherin function. Yet, the fact that approximately 14% of the podoplanin-expressing carcinomas are negative for E-cadherin expression indicates that podoplanin does not necessarily prevent the loss of E-cadherin expression in invasive tumor cells.

We next examined whether the expression of other epithelial markers, such as the cytoplasmic adherens junction proteins β catenin and p120 catenin, was maintained together with E-cadherin at the cell membrane of podoplanin-expressing β tumor cells. No membrane staining for β catenin and p120 catenin was detectable in carcinomas of Rip1Tag2 mice, except for vascular cells within the tumor area (Figures S3A and S3C). In contrast, in the invasive fronts of podoplanin-expressing tumors, together with the continuing expression of E-cadherin, a strong membrane staining for both β catenin and p120 catenin could be detected (Figures S3B and S3D). Analysis of the expression of the tight junction protein ZO-1 revealed comparable results (Figure S4).

Next, we determined whether a cadherin switch, i.e., the switch from E-cadherin to N-cadherin expression, occurred in podoplanin-expressing tumors. In the carcinomas of Rip1Tag2 control mice, expression of E-cadherin was lost and the expression of N-cadherin was strongly upregulated (Figures 3A and 3C). In contrast, in podoplanin-expressing tumors, only a very weak staining for N-cadherin was detectable, while E-cadherin expression remained present (Figures 3B and 3D). Apparently, a switch in cadherin expression is not required for the development of invasive carcinomas in double-transgenic Rip1Podo;Rip1Tag2 mice. Instead, E-cadherin, together with

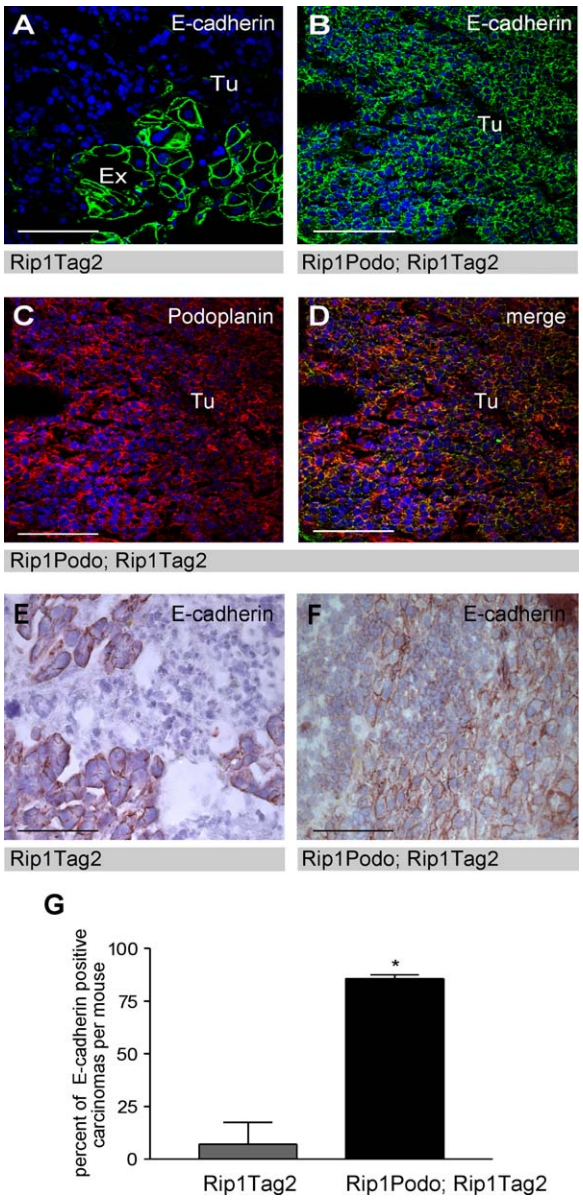

Figure 2. Podoplanin induces tumor invasiveness without loss of E-cadherin expression

A–D: Pancreatic sections from Rip1Tag2 (**A**) and Rip1Podo;Rip1Tag2 (**B**, **C**, and **D**) were stained by immunofluorescence with antibodies against E-cadherin (green) and podoplanin (red) as indicated. Note that the invasive β cell carcinoma of a single-transgenic Rip1Tag2 mouse has lost E-cadherin expression (**A**), whereas podoplanin-expressing tumor cells, despite their apparent invasion into surrounding tissue, maintain the expression of E-cadherin (**B** and **C**). Podoplanin and E-cadherin colocalize at cell membranes in these cells (**D**). Blue staining, DAPI (nuclei).

E and F: Immunohistochemical visualization of E-cadherin expression. E-cadherin expression (brown) is lost in an invasive carcinoma of a Rip1Tag2 mouse, while it is present in the exocrine pancreatic tissue (**E**). In an invasive carcinoma of a Rip1Podo;Rip1Tag2 mouse, E-cadherin expression (brown) is maintained even in the invading front of the tumor (**F**).

G: Quantitation of E-cadherin expression in classified carcinomas of Rip1Tag2 and Rip1Podo;Rip1Tag2 mice. While only 7% of carcinomas in Rip1Tag2 mice showed E-cadherin expression, approximately 86% of the carcinomas of double-transgenic Rip1Podo;Rip1Tag2 mice maintained expression of E-cadherin (*p = 0.0009, Fisher's exact test). Data are shown as mean ± SEM. Ex, exocrine tissue; Tu, tumor tissue. Scale bar = 100 μm.

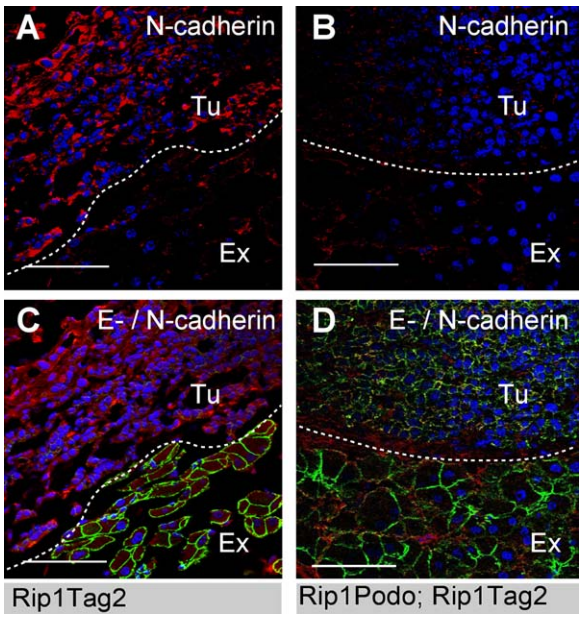

Figure 3. Podoplanin-mediated tumor cell invasion does not involve a cadherin switch

Immunofluorescence staining for N-cadherin (red) (**A** and **B**) and double staining for N-cadherin (red) and E-cadherin (green) (**C** and **D**) on pancreatic sections from Rip1Tag2 (**A** and **C**) and Rip1Podo;Rip1Tag2 (**B** and **D**) mice. Note that in carcinomas of Rip1Tag2 single-transgenic mice, concomitant with the loss of E-cadherin expression, the expression of N-cadherin is upregulated. In contrast, in tumors of Rip1Podo;Rip1Tag2 double-transgenic mice, E-cadherin expression is maintained and N-cadherin is not upregulated. Blue staining, DAPI (nuclei); Ex, exocrine tissue; Tu, tumor tissue. Scale bar = 100 μm.

other adherens and tight junction markers, remains at the membranes of invasive carcinoma cells. These results raise the intriguing possibility that podoplanin is able to induce tumor cell invasion without dissolving epithelial adherens and tight junctions.

Podoplanin relocalizes ERM proteins and rearranges the actin cytoskeleton

Recently, it has been demonstrated that ezrin colocalizes with podoplanin at the cellular membrane in filopodia-like structures (Martin-Villar et al., 2005). Furthermore, ezrin is upregulated in invasive esophageal cancer cells (Shen et al., 2003) and may play a critical role in tumor metastasis (Hunter, 2004). We therefore investigated the distribution of ezrin both in tumors of podoplanin-transgenic mice and in control mice. In invasive tumors of Rip1Tag2 mice, ezrin was localized to the subcortical compartment of the cells, beneath the cellular membrane in the periphery of the cytoplasm (Figure 4A). In tumors of podoplanin-expressing mice, ezrin was redistributed to the edges of invasive tumor cells (Figure 4B). Double staining for ezrin and podoplanin confirmed the relocalization of ezrin and demonstrated a colocalization of podoplanin with ezrin in filopodia-like membrane foci (Figure 4C). Staining for moesin, another ERM protein, showed a comparable pattern (data not shown). Thus, podoplanin overexpression exerts a profound effect on the cellular distribution of ERM proteins, and ERM proteins appear to colocalize with podoplanin in filopodia-like structures at the cell membrane of invasive tumor cells.

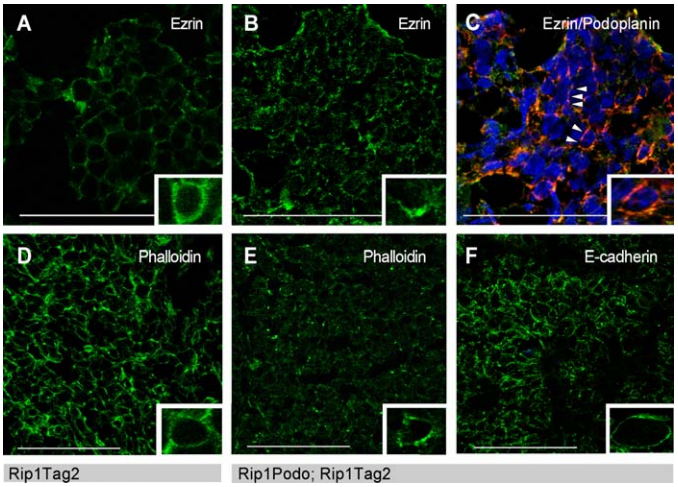

Figure 4. Ezrin and actin filaments are relocalized by podoplanin

A–C: Immunofluorescence staining for ezrin (green) and podoplanin (red) on pancreatic sections of Rip1Tag2 (**A**) and Rip1Podo;Rip1Tag2 (**B** and **C**) mice, as indicated. Note that ezrin is distributed cortically at the cell membrane throughout the tumor of a Rip1Tag2 mouse (**A**), whereas its presence is more irregular with significant localization to focal membrane regions in tumor cells of Rip1Podo;Rip1Tag2 mice (**B**). Double staining of pancreatic sections from Rip1Podo;Rip1Tag2 mice reveals that ezrin (green) and podoplanin (red) colocalize (yellow) at filopodia-like structures at the plasma membrane of podoplanin-expressing β tumor cells, indicated by arrow heads (**C**).

D–F: Fluorescent phalloidin staining for actin (**D** and **E**) and E-cadherin (**F**) on pancreatic sections from Rip1Tag2 (**D**) and Rip1Podo;Rip1Tag2 (**E** and **F**) mice, as indicated. Note the regular subcortical distribution of actin in β tumor cells of Rip1Tag2 mice, yet an irregular pattern with foci of actin accumulation in tumor cells of Rip1Podo;Rip1Tag2 mice. Staining for E-cadherin on adjacent histological sections demonstrates intact cell membranes in the tumor cells of Rip1Podo;Rip1Tag2 mice. Blue staining, DAPI (nuclei). Scale bar = 100 μm.

Inserts in **A**–**F** represent higher magnifications of single cells.

Both ZO-1 and ERM proteins are known to bind and modulate the actin cytoskeleton (McClatchey, 2003; Smalley et al., 2005). To investigate the consequences of podoplanin overexpression on the actin cytoskeleton, we performed fluorescent phalloidin staining on histological sections of tumors from Rip1Tag2 and Rip1Podo;Rip1Tag2 mice. In control mice, staining of actin filaments appeared in the subcortical compartment of the cells (Figure 4D). In podoplanin-expressing tumor cells, actin filament staining was generally reduced, yet a significant subset remained in focal membrane areas, which resemble filopodia (Figure 4E). Proper membrane localization of E-cadherin indicated that the relocalization of actin filaments was not caused by damage to membrane structures in podoplanin-expressing tumor cells (Figure 4F). Taken together, actin filament localization is strongly affected by the presence of podoplanin: subcortical actin filaments are markedly reduced in podoplanin-expressing tumor cells and are relocalized to filopodia-like foci at the plasma membrane.

Podoplanin induces filopodia formation, cell migration, invasion, and spreading in vitro

To investigate whether the upregulated expression of podoplanin affected E-cadherin expression as well as cell morphology and function in cultured tumor cells in vitro, MCF7 breast carcinoma cells were stably transfected with a podoplanin expression construct or with empty vector as control. MCF7 cells are known to express high levels of E-cadherin and to exhibit epithelial morphology. Four control and four podoplanin-transfected clonal cell lines were selected, and the expression of podoplanin was verified by immunoblotting and immunofluorescence analysis (Figure S5A and Figures 5B, 5D, and 5F, respectively). As expected, MCF7-control cells formed epithelial layers with pronounced E-cadherin-mediated adherens junctions. No staining for podoplanin was detectable (Figure 5A). Expression of podoplanin in MCF7-podoplanin cells caused a dramatic change in cellular shape and migratory behavior with the formation of many filopodia-like structures (Figure 5B). Podoplanin was found to be evenly distributed in all plasma membranes. Similar to β tumor cells in Rip1Podo;Rip1Tag2 mice, podoplanin expression did not result in a loss of E-cadherin function, yet colocalization between E-cadherin and podoplanin was restricted to cell-cell junctions where no filopodia-like protrusions were observed (Figure 5B). No upregulation of EMT markers such as N-cadherin or vimentin could be observed in podoplanin-transfected MCF7 cells (Figure S5B). To demonstrate that MCF7 cells were actually able to undergo EMT, we ablated E-cadherin expression in these cells by transfection of a specific antisense shRNA vector (pSuperRetro Ecad). Indeed, upon marked reduction of E-cadherin expression, MCF7 cells upregulated the expression of N-cadherin and vimentin, an indication for EMT (Figure S5B). This finding underlines the observation that podoplanin does not induce a cadherin switch or EMT.

Double staining for podoplanin and ezrin in podoplanin-expressing MCF7 cells confirmed the colocalization of podoplanin and ezrin at the cell membrane of microspikes and filopodia (Figures 5C and 5D). Double staining for podoplanin and phalloidin/actin revealed a dramatic reduction in actin stress fibers in podoplanin-transfected cells, with an evident relocalization of actin to filopodia (Figures 5E, 5F, and 5G). To investigate a direct physical interaction between podoplanin, E-cadherin, ezrin, and actin, we performed immunoprecipitation experiments with specific antibodies against podoplanin. However, none of the aforementioned molecules coprecipitated with podoplanin (data not shown). Yet, these experiments revealed that the phosporylated form of ezrin was much more abundant in podoplanin-transfected cells (Figure 5I), suggesting that podoplanin indirectly affects ezrin function and with it the actin cytoskeleton.

Cell spreading has been shown to be mediated by filopodia formation (Price et al., 1998). To assess whether the filopodia that formed upon the expression of podoplanin were functional, we compared control and podoplanin-transfected cells for their ability to spread on culture dishes precoated with fibronectin. Cell spreading was significantly accelerated in podoplanin-transfected cells (Figures 6A and 6B), which could be repressed by neutralizing antibodies against β_1 integrin (data not shown).

Next, we performed in vitro scratch wounding assays on confluent monolayers of MCF7 cells (Figure S6). With podoplanin-transfected cells, a broad migrating front was visible in the gap after 8 hr, and after 24 hr the gap had closed, whereas with MCF7-control cells, only a few single migrating cells were detectable after 8 hr and the gap had not closed after 24 hr. Rates of cell proliferation were not different between podoplanin-transfected and control cells, excluding any proliferation effects on cell migration (Figure S5C). To determine whether the podoplanin-mediated increase in cell migration was accompanied by cell polarization, the cells in the scratch wounding assays were

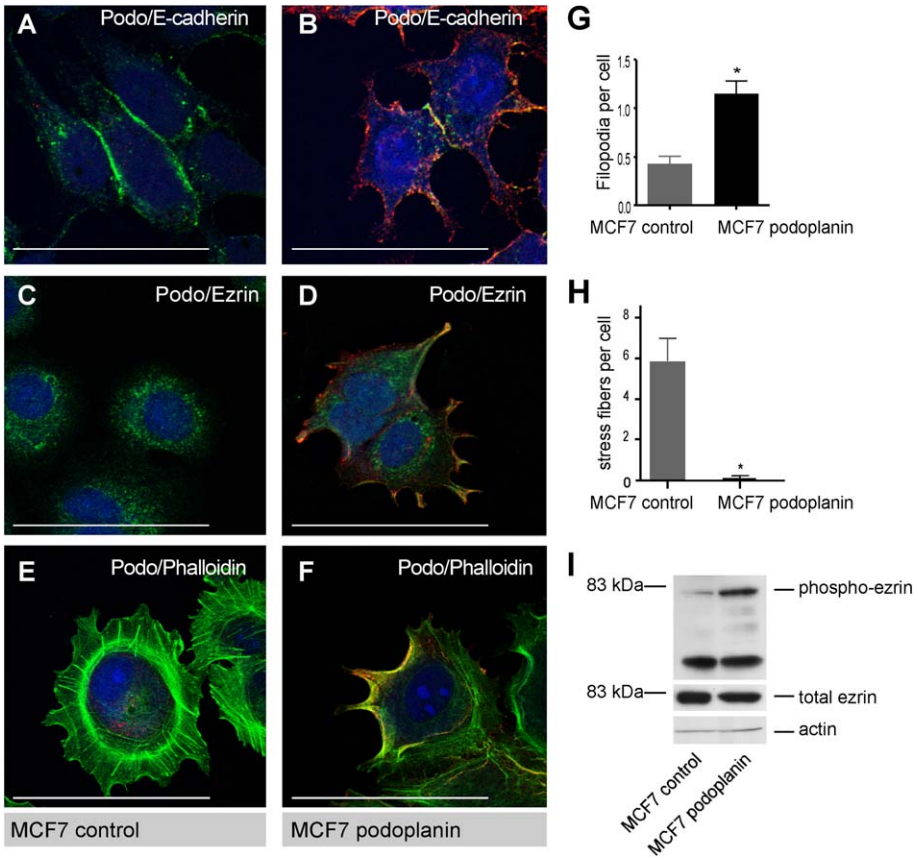

Figure 5. Podoplanin induces a migratory phenotype in MCF7 cells

A: Double staining against podoplanin and E-cadherin in MCF7 control cells does not reveal any podoplanin (red) expression, yet demonstrates high levels of E-cadherin (green) in cell-cell junctions.

B: Expression of podoplanin (red) in MCF7-podoplanin cells does not abrogate E-cadherin (green) expression at cell junctions.

C: Double staining for podoplanin (red) and ezrin (green) reveals a regular, subcortical distribution of ezrin (green) in MCF7-control cells.

D: In contrast, a strong colocalization of both molecules is evident in filopodia-like structures of podoplanin-expressing MCF7 cells (yellow).

E and F: Immunofluorescence staining of podoplanin (red) and actin/phalloidin (green) reveals many stress fibers in MCF7 control cells (**E**), whereas stress fibers are dissolved and actin filaments are redistributed to filopodia-like structures in podoplanin-transfected cells (yellow) (**F**).

G: The number of filopodia (defined as F actin positive membrane protrusion of >5 μm length) is significantly increased in podoplanin-transfected MCF7 cells as compared to control cells (*$p < 0.0001$, two-sided t test).

H: Conversely, the number of stress fibers is dramatically reduced in podoplanin-transfected cells (*$p < 0.0001$, two-sided t test). Data are shown as mean ± SEM.

I: Immunoblotting analysis of ezrin phosphorylation. The level of phospho-ezrin (but not total ezrin) is increased in podoplanin-transfected cells as compared to control MCF7 cells. Scale bar = 20 μm.

stained with antibodies against the specific *cis*-Golgi marker p115 (Gadea et al., 2002). While 25% of the control cells exhibited a polarized orientation of the Golgi apparatus, 42% of podoplanin-expressing cells migrated in a polarized manner ($p < 0.016$, chi-square test).

The effect of podoplanin expression on cell migration and invasion was quantified by two-chamber migration and invasion assays, where podoplanin-expressing and control MCF7 cells were seeded in the upper chamber of transwell inserts and migration of cells along a serum gradient through a membrane was observed. In the invasion assay, transwell membranes were additionally coated with a layer of polymerized matrigel. These experiments revealed that migration of podoplanin-transfected cells was significantly higher as compared to control cells (Figure 6C), and that the invasion rate was even more pronounced in podoplanin-expressing cells as compared to control cells (Figure 6D).

Since the invasive behavior of tumor cells and in particular of cells of the invading front is known to be influenced by growth factors derived from the tumor stroma, we set out to investigate whether podoplanin expression can be induced by stromal factors. MCF7 cells were stimulated for different time periods with FGF2, EGF, TGFβ, IGF1, TNF-α, or HGF, and podoplanin expression was determined by immunoblotting. Of all the factors tested, only EGF markedly upregulated podoplanin expression in MCF7 cells (Figure S5D), while a somewhat weaker induction could be observed with FGF2 and TGFβ (data not shown).

Taken together, the results from these in vitro experiments confirm that the promigratory and proinvasive effect of podoplanin is independent of EMT or a cadherin switch, and is rather due to a dramatic reorganization of the actin cytoskeleton. In podoplanin-transfected cells, the loss of stress fibers is accompanied by the formation of microspikes and filopodia, indicating highly motile cell membranes. As a consequence, these cells exhibit enhanced spreading on extracellular matrix components and increased migratory and invasive capabilities. Thereby, the induction of podoplanin in the invading tumor front may be mediated by stromal growth factors, such as EGF, FGF2, and TGFβ.

Podoplanin downregulates RhoA activity but acts independently of Cdc42

Our results indicate that podoplanin prevents stress fiber formation. Disruption of stress fibers can also be caused by an inactivation of the small GTPase RhoA pathway (Izawa et al., 1998). To test whether RhoA inactivation may be involved in the podoplanin-mediated reduction of stress fiber formation, we transfected control and podoplanin-expressing MCF7 cells with constitutive-active or dominant-negative forms of RhoA (Figure 7A). In addition, we also treated MCF7 cells with Y27632, an inhibitor of the Rho signaling effector, RhoA-associated kinase (Rock). Expression of constitutive-active RhoA efficiently reversed the loss of stress fibers in podoplanin-transfected cells ($p < 0.0001$, one-way ANOVA with Newman-Keuls post-test). Dominant-negative RhoA and the Rock inhibitor Y27632, on the other hand, repressed stress fiber formation in control cells to levels observed in podoplanin-expressing cells. To investigate whether podoplanin-mediated loss of stress fibers was due to an inactivation of RhoA, we performed RhoA activity assays. These experiments revealed a strong downregulation of activated RhoA

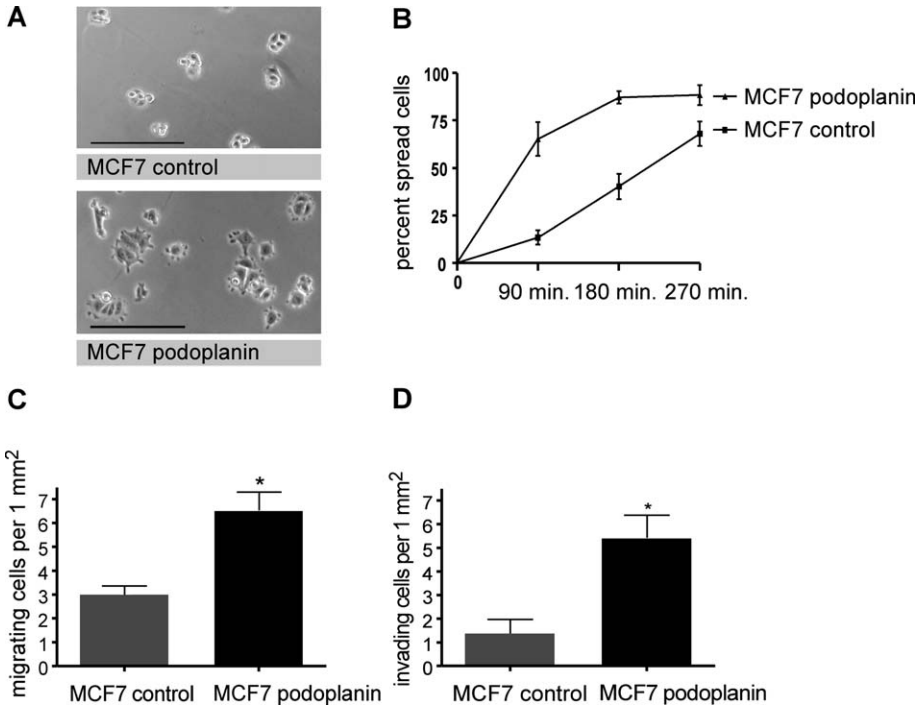

Figure 6. Podoplanin induces spreading, migration, and invasion of MCF7 cells

A and B: Podoplanin-transfected cells showed a markedly accelerated spreading on fibronectin ($p < 0.0001$, Fisher's exact test, for all time points). In addition, more filopodia were detectable in podoplanin cells after 90 min of incubation (compare upper and bottom panel in **A**).

C: The number of migrating MCF7 cells through 8 μm pore transwell filters is significantly increased with the expression of podoplanin (*$p = 0.0072$, two-sided t test).

D: Podoplanin expression also significantly induces invasion of MCF7 cells through a matrigel-coated transwell filter (*$p = 0.0019$, two-sided t test).

Data are representative of four (**B**) or three (**C** and **D**) independent experiments, respectively, and are shown as mean ± SEM.

in podoplanin-transfected cells as compared to control cells (Figure 7C).

In contrast to stress fiber formation by RhoA, the Rho family GTPase Cdc42 and Rac1 are known to induce filopodia and lamellipodia, respectively (Fukata et al., 2003; Sahai and Marshall, 2002). To investigate the mechanisms of filopodia formation in podoplanin-transfected MCF7 cells, we transfected these cells with either constitutive-active Cdc42 or dominant-negative Cdc42. In dominant-negative Cdc42-transfected cells, podoplanin still mediated the formation of filopodia, although a modest reduction in filopodia formation was observed in both podoplanin-expressing and MCF7-control cells (Figure 7B). Conversely, constitutive-active Cdc42 dramatically increased filopodia formation in both cell types. Interestingly, the Rock inhibitor Y27632 also induced filopodia formation in MCF7 control cells (Figure 7B and Figure S7). To verify these results, we performed Cdc42 activity assays, which revealed a significant reduction in Cdc42 activities between podoplanin-transfected and control cells (Figure 7C). Activity assays for Rac1, the third member of the Rho familiy of small GTPases, also showed a downregulation of Rac1 activity upon podoplanin expression (Figure 7C). Yet, transfection of MCF7 and MCF7 podoplanin cells with constitutive-active and dominant-negative Rac1 did not result in a significant change in cell morphology (data not shown). Together, these results suggest that podoplanin-mediated formation of filopodia does not involve the activation of Cdc42 or Rac1. Rather, inhibition of RhoA or Rock activities directly caused the formation of filopodia.

To investigate the functional impact of RhoA downregulation on cell invasion, MCF7 cells stably transfected with constitutive-active RhoA or dominant-negative RhoA or treated with Y27632 were analyzed in a matrigel invasion assay (Figure 7D). Stable expression of constitutive-active RhoA inhibited invasion of control MCF7 cells. Conversely, MCF7 cells transfected with dominant-negative RhoA or treated with Y27632 exhibited markedly increased cell invasion (Figure 7D and Figure S7). These results support the notion that podoplanin induces tumor cell invasion by inhibiting the RhoA pathway. Treatment of both control and podoplanin-transfected MCF7 cells with tissue inhibitor of MMPs (TIMP2), a general MMP inhibitor, almost completely abrogated cellular invasion (Figure 7D).

These results indicate that podoplanin downregulates RhoA activity, thereby ablating stress fibers, inducing filopodia formation, and promoting tumor cell migration and invasion. Thereby, the enhanced invasion properties of podoplanin-expressing cells appear to depend on the activity of MMPs.

Coexpression of podoplanin and E-cadherin in the invasive front of human cancer

To investigate whether podoplanin possesses an invasion-inducing function in human cancers, histological sections of squamous cell carcinomas (from esophagus, skin, larynx, cervix, and lung) and adenocarcinomas (from lobular breast cancer, prostate, and colon) were stained with antibodies against podoplanin (red) and E-cadherin (brown) (Figure 8). A total of 189 tumor fronts were analyzed. Approximately 80% of the investigated tissue samples of human squamous cell cancers of the lung, skin, esophagus, larynx, and cervix expressed podoplanin. Notably, in all these samples, podoplanin expression was restricted to the outer cell layer of the invading tumor fronts (Figures 8A–8E). Similar to podoplanin-expressing β tumor cells and MCF7 cells, podoplanin and E-cadherin were coexpressed in the invasive front of squamous cell carcinomas (Figures 8A–8E). In contrast to squamous cell carcinomas, adenocarcinomas did not express podoplanin in their invading fronts, although E-cadherin expression was partially maintained in the tumor tissue samples analyzed. The notable exception was lobular breast cancer, which coexpressed podoplanin together with E-cadherin in areas of the invading front (Figure 8F). The results of the analysis of human cancer biopsies suggest an important

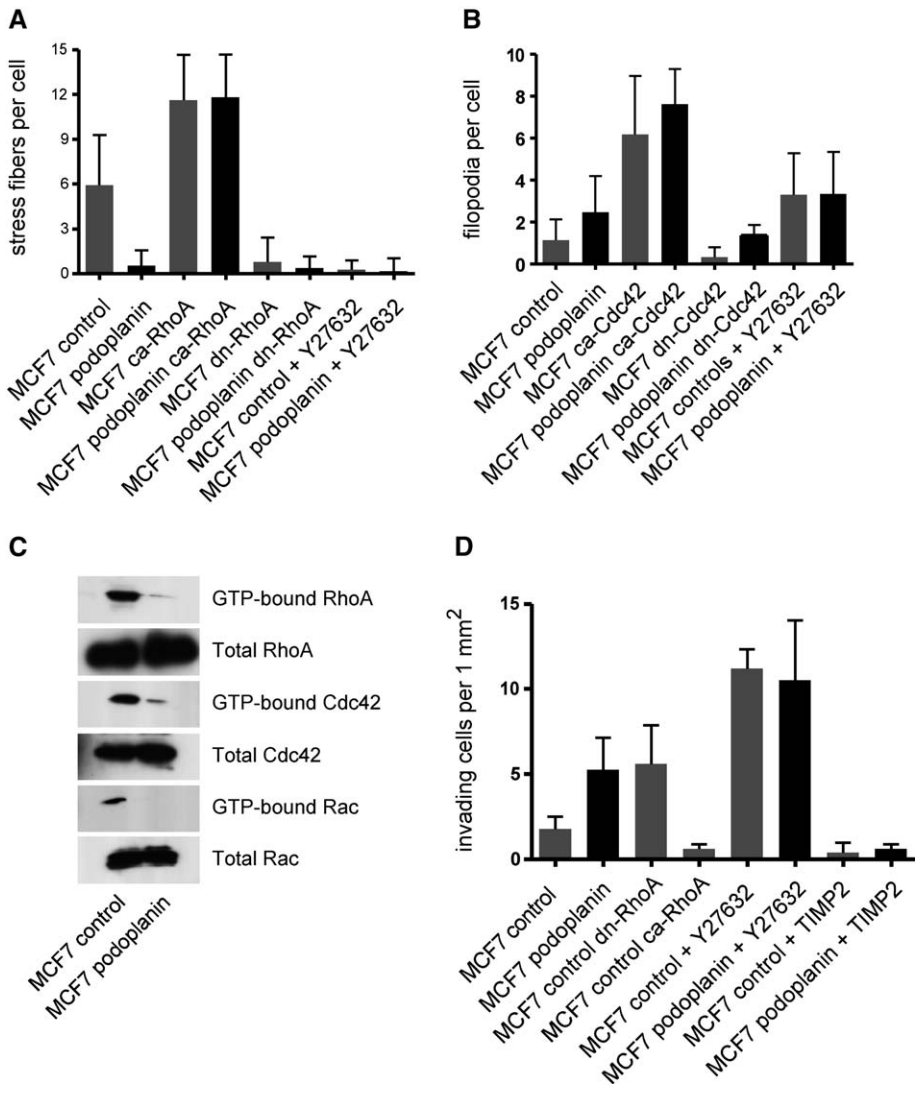

Figure 7. Podoplanin downregulates RhoA, Cdc42, and Rac activity

A: Expression of podoplanin represses stress fiber formation in MCF7 cells. Expression of dominant-negative RhoA (dn-RhoA) abrogates stress fiber formation in control-transfected cells, indicating that RhoA activity is required for stress fiber formation in MCF7 cells. Expression of constitutive-active RhoA (ca-RhoA) increases the number of stress fibers in both control and podoplanin-transfected cells. The Rock inhibitor Y27632 inhibits the formation of stress fibers in MCF7 cells.

B: Podoplanin induces filopodia formation. Transfection of constitutive-active Cdc42 (ca-Cdc42) in control- and podoplanin-transfected cells results in a strong increase in the number of filopodia. Transfection of dominant-negative Cdc42 (dn-Cdc42) in podoplanin-transfected cells does not significantly affect filopodia formation, whereas the Rock inhibitor Y27632 induces filopodia formation in MCF7 control cells.

C: Analysis of RhoA, Cdc42, and Rac1 GTPase activity by GST-C21 and GST-PAK pulldown assays, respectively. Note that podoplanin expression strongly reduces RhoA, Cdc42, and Rac1 activities.

D: Invasion of MCF7 cells is promoted if cells are transfected with podoplanin or dominant-negative RhoA or are treated with the Rock inhibitor Y27632. Invasion of MCF7 cells is reduced if cells are transfected with constitutive-active RhoA. Upon treatment with TIMP2, invasion is markedly reduced in both podoplanin-expressing and control MCF7 cells.

Data are shown as mean ± standard deviation.

role for podoplanin in the progression of squamous cell carcinomas and possibly of specific adenocarcinomas. Apparently, human squamous cell carcinomas reveal a phenotype of large invading tumor fronts without microinvasion, which corresponds to the phenotype of collective cell migration (Friedl and Wolf, 2003).

Together, the experimental results from human cancer biopsies, cultured MCF7 breast cancer cells, and the Rip1Tag2 mouse model of carcinogenesis indicate that upregulated expression of podoplanin is causing tumor cell invasion by a pathway that is independent of EMT or the ablation of E-cadherin function. It most likely acts via specific changes in RhoA signaling, in the organization of ERM proteins, and the actin cytoskeleton, and, as a result, mediates collective cell migration in cancers with conelike invasion patterns.

Discussion

Recently, it has been reported that podoplanin expression is upregulated in different human cancers, suggesting a role for podoplanin in tumor progression (Schacht et al., 2005). Here, we employed a transgenic mouse model of carcinogenesis, cultured human breast cancer cells, and biopsies from cancer patients to investigate the functional contribution of podoplanin to tumor progression. Transgenic expression of podoplanin in Rip1Tag2 transgenic mice caused an acceleration of tumor progression with a higher incidence of tumor invasion and tumor malignancy, without the formation of lymph node or distant organ metastasis.

The presence of podoplanin during tumor progression in Rip1Tag2 mice had a rather unexpected impact on cell adhesion molecules in β tumor cells. Notably, expression of the epithelial adherens junction protein E-cadherin and its cytoplasmic linker molecules β catenin and p120 catenin and the tight junction protein ZO-1 was maintained during the progression from a benign tumor (adenoma) to an invasive tumor (carcinoma) in double-transgenic Rip1Podo;Rip1Tag2 mice. In addition, we could not detect any upregulation of N-cadherin or any other mesenchymal marker in the invasive tumors of double-transgenic mice. This is surprising, since the loss of E-cadherin has been shown to be a rate-limiting step in the transition from adenoma to carcinoma in Rip1Tag2 single-transgenic mice (Perl et al., 1998). Apparently, podoplanin is able to induce tumor cell invasion without the need for a cadherin switch or epithelial-mesenchymal transition (EMT).

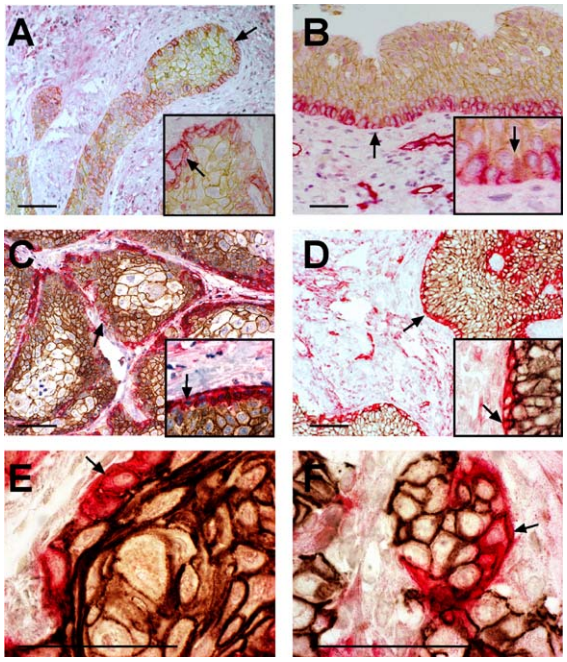

Figure 8. Podoplanin and E-cadherin are coexpressed in the invasive front of human cancers

Immunohistochemical staining for podoplanin (red) and E-cadherin (brown) reveals high expression of both molecules in the invading front of (**A**) invasive human esophageal carcinoma, (**B**) human skin squamous cell cacinoma, (**C**) human larynx carcinoma, (**D**) human cervix carcinoma, (**E**) human lung squamous cell carcinoma, and (**F**) human lobular breast cancer. Whereas E-cadherin is expressed in all carcinoma cells, podoplanin is detectable exclusively in the outer cell layer of the invading front. Inserts: 10× higher magnification of the panel showing coexpression of E-cadherin (brown) and podoplanin (red) in cells of the invasive tumor front (arrows). Scale bar = 50 μm.

Consistent with this intriguing observation, immunohistochemical analysis of squamous cell cancers of the lung, skin, esophagus, larynx, and cervix of cancer patients revealed expression of podoplanin in the invading tumor front in the presence of E-cadherin. In addition, podoplanin was also expressed in human lobular breast cancer. Notably, podoplanin was found to be exclusively expressed in the outer cell layer of the invasive tumor front, whereas E-cadherin was found in both the podoplanin-expressing cancer cells and the inner cells of the invasive tumor front. This particular localization of podoplanin expression raises the question of whether factors secreted from stromal cells can induce podoplanin expression. Indeed, we found that EGF, FGF2, and TGFβ can upregulate expression of podoplanin in MCF7 cells, raising the possibility that stroma-derived growth factors may induce the specific expression of podoplanin in the invading tumor front.

Together, the results demonstrate that overexpression of podoplanin (1) induces filopodia formation and cell polarization, (2) enhances β_1-integrin mediated cell spreading and adhesion on extracellular matrix, (3) leads to increased cell invasion which is dependent on the action of MMPs, and (4) increases cell migration. These processes resemble the steps necessary for collective cell migration as recently described (Friedl et al., 2004; Friedl and Wolf, 2003). In the case of collective cell migration, epithelial markers, E-cadherin-mediated cell-cell adhesion, and β integrin-mediated cell-matrix adhesion are maintained, while EMT does not occur. Many human cancers, including most squamous cell carcinomas and a few adenocarcinomas, exhibit such a histological phenotype of collective cell migration. Here, we have shown that E-cadherin is coexpressed with podoplanin in the invasive front of most human squamous cell carcinomas. Such organization of an invading sheet of cells is not only present in the mouse model and the human cancer biopsies, but is also observed in podoplanin-expressing MCF7 cells: while the cells seem to adhere by their rear ends via E-cadherin-mediated adhesion to their next neighbor, they display filopodia on their invading fronts. This observation is also consistent with the fact that podoplanin-expressing MCF7 cells migrate as a front and not as single cells in scratch wounding assays (Figure S6). Thereby, the cells exhibit polarized migration, as determined by the reorientation of the Golgi apparatus (data not shown). Taken together, these results strongly suggest that podoplanin mediates a novel molecular pathway of collective cell migration. This mechanism stands in contrast to the invasion of single disseminating tumor cells, a process that in most cases involves a cadherin switch and EMT. While the latter process certainly promotes metastasis formation, the contribution of podoplanin-mediated collective cell migration to the metastatic process remains to be determined.

A first analysis of the signaling events that may underlie podoplanin-induced tumor invasion reveals that the activity of the small GTPase RhoA is reduced in podoplanin-expressing cells, which also lack stress fibers. Conversely, stress fibers of podoplanin-transfected cells could be reconstituted by the expression of a constitutive-active from of RhoA, suggesting that podoplanin is acting upstream of RhoA. Unexpectedly, the activity of Cdc42, which is known to play an important role in filopodia formation, is not upregulated by podoplanin. Moreover, the expression of a dominant-negative form of Cdc42 does not significantly repress podoplanin-induced filopodia formation, suggesting a pathway that induces filopodia independently of Cdc42 activity. Podoplanin-mediated downregulation of Rho activity is sufficient to induce filopodia formation and increased cell migration: inhibition of Rho activity by the expression of a dominant-negative form of RhoA or by an inhibitor of the RhoA effector kinase Rock promotes filopodia formation. Rac activity is also downregulated in podoplanin transfected cells, but seems to be without functional relevance for the cellular parameters analyzed in MCF7 cells.

Here, we report a distinct function for podoplanin, the induction of collective cell migration and invasion in the absence of EMT. One major molecular change detected upon podoplanin expression is the combined inactivation of all three major Rho family GTPases, RhoA, Rac1, and Cdc42, a constellation that thus far has not been reported in any specific cellular context. We can only speculate on the molecular mechanisms by which podoplanin modulates such repression and how the loss of RhoA activity actually leads to filopodia formation and cell migration and invasion. Podoplanin is highly glycosylated on its extracellular domain, and the intracellular terminus consists of only nine amino acids. Moreover, there is no apparent homology to any other protein domains and, hence, podoplanin may act by novel molecular pathways involving as yet unknown binding partners, including soluble ligands or cell surface molecules interacting with podoplanin's carbohydrate moiety or signaling effector molecules at the inside of the cell. However, immunoprecipitation experiments did not reveal any direct binding partner

of podoplanin. The significant colocalization of ezrin and podoplanin in filopodia-like structures together with increased phosphorylation of ezrin in podoplanin-expressing cells suggest that ERM proteins may play a major role in podoplanin's modulation of the actin cytoskeleton. The Rho family of small GTPases exerts multiple effects on the phosphorylation of ERM proteins: RhoA and Cdc42 are thought to promote, and Rac to inhibit, ERM protein phosporylation (Ivetic and Ridley, 2004, Matsui et al., 1998). However, in our experiments, the activities of all three Rho GTPases are found to be downregulated, whereas ezrin is highly phosphorylated. Hence, whether the increased phosphorylation of ezrin and other ERM proteins is due to an overall repression of Rho GTPase activities or involves a hitherto unknown pathway, mediated by podoplanin, remains to be elucidated.

Database expression analyses did not identify any established carcinoma cell line that expressed significant amounts of podoplanin, thus excluding siRNA knockdown experiments which would be important in further investigating podoplanin's tumor invasive function. Moreover, since podoplanin knockout mice are not viable (Schacht et al., 2003), conditional knockout approaches will have to be employed to ablate podoplanin function in mouse models of tumorigenesis in vivo.

In conclusion, we hypothesize that podoplanin induces collective tumor cell invasion in the absence of a cadherin switch or EMT. Unraveling the molecular details of this process and identifying the signaling molecules and pathways involved in it may have a major impact on cancer diagnosis and therapy and, thus, deserve future research.

Experimental procedures

Transgenic mice

Rip1Podo transgenic mice were generated according to standard procedures (Labosky et al., 1994). The entire coding region of mouse podoplanin was amplified by RT-PCR using the primer pair 5′-gcaattctagaatgtggaccgtgc cag-3 and 5′-gcaataagcttttagggcgagaaccttc-3 and mouse kidney cDNA as template and cloned under the control of the rat insulin gene II promoter (Rip1; Hanahan, 1985). The genotypes of six founder mice were confirmed by Southern blot and PCR analysis. Transgene expression was confirmed by RT-PCR and immunohistochemical and immunoblotting analysis. One podoplanin-expressing mouse line, with approximately 23 inserted transgene copies, was used for further experimentation. Generation and phenotypic characterization of Rip1Tag2 mice has been described previously (Hanahan, 1985). Rip1Podo female mice were crossed with Rip1Tag2 male mice to generate double-transgenic Rip1Podo;Rip1Tag2 mice. Mice were kept in a strict C57Bl/6 background. PCR primers were: Rip1Podo: 5′-CTGCAGCTTCA GCCCCTCTG-3′ and 5′-CTGGCACGGTCCACATTCTAG-3′; Rip1Tag2: 5′-GGACAAACCACAACTAGAATGGCAG-3′ and 5′-CAGAGCAGAATTGTGGA GTGG-3′.

All experiments performed with mice were in accordance with the guidelines of the Swiss Federal Veterinary Office (SFVO) and the regulations of the Cantonal Veterinary Office of Basel-Stadt.

Histopathological analysis

Mice were sacrificed at 12 weeks of age. Tumor number and diameter were measured, and tumor volumes were calculated assuming a spherical shape of the tumors. The preparation of paraffin and frozen tissue sections and immunohistochemical and immunofluorescent analysis was performed as described previously (Perl et al., 1998). The following primary antibodies were used at the dilutions indicated: hamster anti-mouse podoplanin, 1:500 (8.1.1, DSHB, Iowa University); rabbit anti-human podoplanin, 1:100 (Breiteneder-Geleff et al., 1999); rat anti-E-cadherin, 1:100 (Zymed, San Diego, California); mouse anti-N-cadherin, 1:100 (Zymed, San Diego, California); rabbit anti-β catenin, 1:150 (Sigma, St. Louis, Missouri); mouse anti-p120 catenin, 1:150 (Transduction Laboratories, San Jose, California); rat anti-CD31, 1:100 (BD Biosciences, San Jose, California); mouse anti-moesin, 1:100 (BD Biosciences, San Jose, California); mouse anti-ezrin, 1:100 (BD Biosciences, San Jose, California); rabbit anti-phospho-ezrin/radixin/moesin (Chemicon, Dietkon, Switzerland); rat anti-ZO-1, 1:100 (Chemicon, Temecula, California); goat anti-insulin, 1:50 (Dako, Baar, Switzerland); rabbit anti-glucagon, 1:50 (Linco, St. Charles, USA); Alexa fluor 488 phalloidin, 1:50 (Molecular Probes, San Diego, California). In case of mouse anti-mouse antibodies, background was reduced by additional blocking with the m.o.m. kit (Vector Laboratories, Burlingame, California). Staining was evaluated on an AxioVert and a LSM 510 META confocal microscope (Zeiss, Oberkochen, Germany). Histological staging and grading was done in a blindfold manner and repeated twice.

MCF7 cell transfection and induction experiment

A cDNA fragment encoding human podoplanin was subcloned into pIRES (Clontech, Mountain View, California). Constitutive-active and dominant-negative Cdc42, RhoA, and Rac1 cloned in pTriEx-4 (Kinexus, Vancouver, Canada) were a generous gift from O. Pertz (The Scripps Research Institute, La Jolla, California). Vectors and empty vector controls were transfected into MCF7 cells using the Amaxa electroporation system following the manufacturer's instructions (Amaxa, Köln, Germany). Cells were selected in 750 μg/ml G418. Transient transfections of MCF7 cells were performed with Fugene (Roche, Basel, Switzerland). Cells grown on a coverslip were fixed in 4% paraformaldehyde for 15 min, incubated with 0.2% Triton-X for 2 min, washed in PBS, blocked with 5% goat serum for 15 min, and stained with the appropriate primary and secondary antibodies as described above.

Immunoblotting

For total cell lysates, cells were lysed at 4ºC in RIPA-plus buffer (50 mM Tris-Hcl [pH 8], 150 mM NaCl, 2 mM $MgCl_2$, 2 mM $CaCl_2$, 0.5% NaDoc, 10% glycerol, 1% NP40, 0.1% SDS, 1 mM NaF, 2 mM $NaVO_4$, 0.1 mM PMSF, 1 mM DTT, and protease inhibitor cocktail). 30 μg of cleared protein lysates were separated by SDS-PAGE and electroblotted on PDVF membranes, and proteins were visualized with the appropriate primary and secondary antibodies and ECL (Amersham, Otelfingen, Switzerland) on superRX films (Fuji, Dielsdorf, Switzerland).

Migration and invasion assays

Cell migration was determined by using a modified two-chamber migration assay (Falcon BD, Franklin Lakes, New Jersey) with a pore size of 8 μm. For the invasion assay, the membrane was coated with 20 μl of a 2.5 mg/ml solution of matrigel (Falcon BD). For both assays, 10^5 MCF7 cells were seeded in 1% fetal calf serum/DMEM medium (Sigma, St. Louis, Missouri) in the upper chamber, and the lower chamber was filled with 10% fetal calf serum/DMEM medium. After 24 hr incubation at 37ºC, cells in the upper chamber were carefully removed with a cotton swab and the cells that had traversed the membrane were fixed in 4% paraformaldehyde/HBS-Ca^{2+}, stained with crystal violet (0.5% in 20% methanol), and counted. For functional assays, the Rock inhibitor Y27632 (Sigma Aldrich, Basel) and the tissue inhibitor of matrix metalloproteases 2 (TIMP2, a kind gift of A. Noel, Liege, Belgium) were added to the cell suspensions at a concentration of 10 μM and 200 nM, respectively.

Cell spreading assay

To determine cell spreading on fibronectin, 24-well plates were coated with 15 μg/ml fibronectin (Sigma, St. Louis, Missouri). 10^4 cells were then plated in low serum medium (1% FCS in DMEM), and 30 min after seeding, the medium was changed to eliminate unattached cells. Cells were incubated at 37ºC and monitored in regular intervals. Adherent cells were photographed under phase contrast and counted as flattened or round cells. Cell spreading was confirmed in four independent experiments.

RhoA, Cdc42, and Rac activity assay

The RhoA, Cdc42, and Rac activity assays were performed as described (Sander et al., 1999). Briefly, 5×10^6 cells were lysed before incubation with GST-PAK (for Cdc42 and Rac) or GST-C21 fusion protein (for RhoA). After precipitation, complexes were washed with lysis buffer, resolved by SDS-PAGE, immunoblotted, and analyzed with antibodies against RhoA, Cdc42, and Rac (Transduction Laboratories, San Jose, California).

Statistical analysis

Statistical analysis and graphs were performed with GraphPad Prism software (GraphPad Software Inc., San Diego, USA). Fisher's exact test was used for the binomial analysis of the adenoma and carcinoma frequency, E-cadherin presence or absence in carcinomas, and flattened or round cells in the cell spreading assay. The chi-square test was employed to statistically analyze carcinoma gradings. Statistical analysis of the incidence of MCF7 cell filopodia as well as the quantification of MCF7 cell migration and invasion was done by unpaired, two-sided t test. Normality testing was performed using the Kolmogorov-Smirnov test with Dallal-Wilkinson-Lilliefor p value.

Supplemental data

The Supplemental Data include Supplemental Experimental Procedures and seven supplemental figures and can be found with this article online at http://www.cancercell.org/cgi/content/full/9/4/261/DC1/.

Acknowledgments

The authors are grateful to C. Theussl, K. Strittmatter, S. Schoppmann, E. Gurnhofer, H. Höger, U. Schmieder, H. Antoniadis, and R. Jost for technical support and advice. We thank T. Schomber, A. Fantozzi, and M. Cabrita for critical input on the manuscript, and O. Pertz (The Scripps Research Institute, La Jolla, California), H. Kowalski (Clinical Institute of Pathology, Medical University of Vienna), A. Noel (University of Liege, Belgium), and G. Orend (Institute for Biochemistry and Genetics, University of Basel) for providing plasmids and reagents. This work was supported by the Roche Research Foundation (A.W.), the EU-FP6 framework program LYMPHANGIOGENOMICS LSHG-CT-2004-503573 (D.K. and G.C.), the Center of Excellence in Clinical and Experimental Oncology (CLEXO) of the General Hospital and Medical University of Vienna (D.K.), the EU-FP6 framework program BRECOSM LSHC-CT-2004-503224 (G.C.), and the Swiss Bridge Award (G.C.).

Received: September 20, 2005
Revised: December 21, 2005
Accepted: March 10, 2006
Published: April 10, 2006

References

Breiteneder-Geleff, S., Soleiman, A., Kowalski, H., Horvat, R., Amann, G., Kriehuber, E., Diem, K., Weninger, W., Tschachler, E., Alitalo, K., and Kerjaschki, D. (1999). Angiosarcomas express mixed endothelial phenotypes of blood and lymphatic capillaries: podoplanin as a specific marker for lymphatic endothelium. Am. J. Pathol. *154*, 385–394.

Cavallaro, U., and Christofori, G. (2004). Cell adhesion and signalling by cadherins and Ig-CAMs in cancer. Nat. Rev. Cancer *4*, 118–132.

Cavallaro, U., Schaffhauser, B., and Christofori, G. (2002). Cadherins and the tumour progression: is it all in a switch? Cancer Lett. *176*, 123–128.

Christofori, G., Naik, P., and Hanahan, D. (1994). A second signal supplied by insulin-like growth factor II in oncogene-induced tumorigenesis. Nature *369*, 414–418.

Farr, A.G., Berry, M.L., Kim, A., Nelson, A.J., Welch, M.P., and Aruffo, A. (1992). Characterization and cloning of a novel glycoprotein expressed by stromal cells in T-dependent areas of peripheral lymphoid tissues. J. Exp. Med. *176*, 1477–1482.

Folkman, J., Watson, K., Ingber, D., and Hanahan, D. (1989). Induction of angiogenesis during the transition from hyperplasia to neoplasia. Nature *339*, 58–61.

Friedl, P., and Wolf, K. (2003). Tumour-cell invasion and migration: diversity and escape mechanisms. Nat. Rev. Cancer *3*, 362–374.

Friedl, P., Hegerfeldt, Y., and Tusch, M. (2004). Collective cell migration in morphogenesis and cancer. Int. J. Dev. Biol. *48*, 441–449.

Fukata, M., Nakagawa, M., and Kaibuchi, K. (2003). Roles of Rho-family GTPases in cell polarisation and directional migration. Curr. Opin. Cell Biol. *15*, 590–597.

Gadea, G., Lapasset, L., Gauthier-Rouviere, C., and Roux, P. (2002). Regulation of Cdc42-mediated morphological effects: a novel function for p53. EMBO J. *21*, 2373–2382.

Gonzalez, R.F., and Dobbs, L.G. (1998). Purification and analysis of RTI40, a type I alveolar epithelial cell apical membrane protein. Biochim. Biophys. Acta *1429*, 208–216.

Grunert, S., Jechlinger, M., and Beug, H. (2003). Diverse cellular and molecular mechanisms contribute to epithelial plasticity and metastasis. Nat. Rev. Mol. Cell Biol. *4*, 657–665.

Hanahan, D. (1985). Heritable formation of pancreatic beta-cell tumours in transgenic mice expressing recombinant insulin/simian virus 40 oncogenes. Nature *315*, 115–122.

Hsu, M.Y., Wheelock, M.J., Johnson, K.R., and Herlyn, M. (1996). Shifts in cadherin profiles between human normal melanocytes and melanomas. J. Investig. Dermatol. Symp. Proc. *1*, 188–194.

Hunter, K.W. (2004). Ezrin, a key component in tumor metastasis. Trends Mol. Med. *10*, 201–204.

Ivetic, A., and Ridley, A.J. (2004). Ezrin/radixin/moesin proteins and Rho GTPase signalling in leucocytes. Immunology *112*, 165–176.

Izawa, I., Amano, M., Chihara, K., Yamamoto, T., and Kaibuchi, K. (1998). Possible involvement of the inactivation of the Rho-Rho-kinase pathway in oncogenic Ras-induced transformation. Oncogene *17*, 2863–2871.

Kato, Y., Kaneko, M., Sata, M., Fujita, N., Tsuruo, T., and Osawa, M. (2005). Enhanced Expression of Aggrus (T1alpha/Podoplanin), a Platelet-Aggregation-Inducing Factor in Lung Squamous Cell Carcinoma. Tumour Biol. *26*, 195–200.

Kimura, N., and Kimura, I. (2005). Podoplanin as a marker for mesothelioma. Pathol. Int. *55*, 83–86.

Labosky, P.A., Barlow, D.P., and Hogan, B.L. (1994). Embryonic germ cell lines and their derivation from mouse primordial germ cells. Ciba Found. Symp. *182*, 157–168.

Martin-Villar, E., Scholl, F.G., Gamallo, C., Yurrita, M.M., Munoz-Guerra, M., Cruces, J., and Quintanilla, M. (2005). Characterization of human PA2.26 antigen (T1alpha-2, podoplanin), a small membrane mucin induced in oral squamous cell carcinomas. Int. J. Cancer *113*, 899–910.

Matsui, T., Maeda, M., Doi, Y., Yonemura, S., Amano, M., Kaibuchi, K., and Tsukita, S. (1998). Rho-kinase phosphorylates COOH-terminal threonines of ezrin/radixin/moesin (ERM) proteins and regulates their head-to-tail association. J. Cell Biol. *140*, 647–657.

McClatchey, A.I. (2003). Merlin and ERM proteins: unappreciated roles in cancer development? Nat. Rev. Cancer *3*, 877–883.

Mohr, U., Capen, C.C., Dungworth, D.L., Greaves, P., Hardisty, J.F., Hayashi, Y., Ito, N., Long, P.H., and Krinke, G. (2001). International Classification of Rodent Tumors: Part II, The Mouse (Berlin: Springer).

Noren, N.K., Liu, B.P., Burridge, K., and Kreft, B. (2000). p120 catenin regulates the actin cytoskeleton via Rho family GTPases. J. Cell Biol. *150*, 567–580.

Nose, K., Saito, H., and Kuroki, T. (1990). Isolation of a gene sequence induced later by tumor-promoting 12-O-tetradecanoylphorbol-13-acetate in mouse osteoblastic cells (MC3T3–E1) and expressed constitutively in ras-transformed cells. Cell Growth Differ. *1*, 511–518.

Perl, A.K., Wilgenbus, P., Dahl, U., Semb, H., and Christofori, G. (1998). A causal role for E-cadherin in the transition from adenoma to carcinoma. Nature *392*, 190–193.

Price, L.S., Leng, J., Schwartz, M.A., and Bokoch, G.M. (1998). Activation of Rac and Cdc42 by integrins mediates cell spreading. Mol. Biol. Cell *9*, 1863–1871.

Rishi, A.K., Joyce-Brady, M., Fisher, J., Dobbs, L.G., Floros, J., VanderSpek, J., Brody, J.S., and Williams, M.C. (1995). Cloning, characterization, and development expression of a rat lung alveolar type I cell gene in embryonic endodermal and neural derivatives. Dev. Biol. *167*, 294–306.

Sahai, E., and Marshall, C.J. (2002). RHO-GTPases and cancer. Nat. Rev. Cancer *2*, 133–142.

Sander, E.E., ten Klooster, J.P., van Delft, S., van der Kammen, R.A., and Collard, J.G. (1999). Rac downregulates Rho activity: reciprocal balance between both GTPases determines cellular morphology and migratory behavior. J. Cell Biol. *147*, 1009–1022.

Schacht, V., Ramirez, M.I., Hong, Y.K., Hirakawa, S., Feng, D., Harvey, N., Williams, M., Dvorak, A.M., Dvorak, H.F., Oliver, G., and Detmar, M. (2003). T1alpha/podoplanin deficiency disrupts normal lymphatic vasculature formation and causes lymphedema. EMBO J. *22*, 3546–3556.

Schacht, V., Dadras, S.S., Johnson, L.A., Jackson, D.G., Hong, Y.K., and Detmar, M. (2005). Up-regulation of the lymphatic marker podoplanin, a mucin-type transmembrane glycoprotein, in human squamous cell carcinomas and germ cell tumors. Am. J. Pathol. *166*, 913–921.

Shen, Z.Y., Xu, L.Y., Chen, M.H., Li, E.M., Li, J.T., Wu, X.Y., and Zeng, Y. (2003). Upregulated expression of Ezrin and invasive phenotype in malignantly transformed esophageal epithelial cells. World J. Gastroenterol. *9*, 1182–1186.

Siegel, P.M., and Massague, J. (2003). Cytostatic and apoptotic actions of TGF-beta in homeostasis and cancer. Nat. Rev. Cancer *3*, 807–821.

Smalley, K.S., Brafford, P., Haass, N.K., Brandner, J.M., Brown, E., and Herlyn, M. (2005). Up-regulated expression of zonula occludens protein-1 in human melanoma associates with N-cadherin and contributes to invasion and adhesion. Am. J. Pathol. *166*, 1541–1554.

Thiery, J.P. (2002). Epithelial-mesenchymal transitions in tumour progression. Nat. Rev. Cancer *2*, 442–454.

Zimmer, G., Lottspeich, F., Maisner, A., Klenk, H.D., and Herrler, G. (1997). Molecular characterization of gp40, a mucin-type glycoprotein from the apical plasma membrane of Madin-Darby canine kidney cells (type I). Biochem. J. *326*, 99–108.

Zimmer, G., Oeffner, F., Von Messling, V., Tschernig, T., Groness, H.J., Klenk, H.D., and Herrler, G. (1999). Cloning and characterization of gp36, a human mucin-type glycoprotein preferentially expressed in vascular endothelium. Biochem. J. *341*, 277–284.